Construction and Building Materials 264 (2020) 120152

Contents lists available at ScienceDirect

Construction and Building Materials

journal homepage: www.elsevier.com/locate/conbuildmat

High-performance concrete incorporating calcined kaolin clay and limestone as cement substitute

Hongjian Du *, Sze Dai Pang

Department of Civil and Environmental Engineering, National University of Singapore, 117576 Singapore, Singapore

HIGHLIGHTS

- Calcined clay and limestone are used to replace cement in high-performance concrete.
- Calcined clay starts its pozzolanic reaction prior to the synergy with limestone.
- Higher autogenous shrinkage was recorded for blended cement mixes.
- After 1-week, blended mixes exhibited similar strength with the reference mix.
- Transport of moisture and liquid is greatly hindered by the refined microstructure.

ARTICLE INFO

Article history:
Received 14 April 2020
Received in revised form 18 June 2020
Accepted 5 July 2020

Keywords:
Sustainability
Pozzolanic reaction
Hydration
Strength
Shrinkage
Durability

ABSTRACT

This paper presents a comprehensive study on the properties of high-performance concrete produced with calcined kaolin clay and limestone at cement replacement level of 30% and 45% respectively. A medium-grade kaolin clay was used for thermal treatment at 800 °C. The hydration, strength, shrinkage and transport properties were assessed up to 6 months. Calorimetry, XRD and TG results revealed that the pozzolanic reaction of calcined clay and its synergetic effect with limestone would occur within the first week. Higher autogenous shrinkage was clearly noted. The produced C-A-S-H gels and carbonaluminate phases could effectively enhance the compressive strength and elastic modulus from 7 days onwards. Meanwhile, concrete's resistance against moisture and liquid ingress was found to significantly increase as a result of the more tortuous pathways. The comparable mechanical properties and superior durability performances confirm the viability of realizing high-performance concrete using high content of clay and limestone.

1. Introduction

Production of cement accounts for 5–8% of man-made CO_2 emissions. As the world's growing population and need for habitation drive concrete demand, the associated carbon emissions are consequently set to rise. Burning coals to generate the heat required as well as the chemical process of limestone decomposition are the main sources of carbon emissions in cement production. On average 0.8–0.9 ton of CO_2 is emitted in the production of 1 ton of ordinary Portland cement. Due to the huge amounts of concrete produced and used globally, being able to reduce the carbon emissions per ton of concrete produced would make a significant contribution to controlling global carbon emission [1].

In order to reduce carbon emissions, alternative fuel technologies and energy efficiency have been studied in great detail and may be reaching a plateau of optimization due to technological constraints. An alternate solution that has yet to be fully maximized would be to make use of supplementary cementitious material (SCM) to partially substitute cement clinker in concrete. Some of the more widely used SCMs include fly ash, slags, silica fume, etc. However, existing reserves and production forecast of these industrial by-products will not meet the projected demand for cement [2–4]. Reserves of natural pozzolans such as volcanic ashes are conditioned by local geology and its availability is restricted to only certain geographical locations [5]. In contrast, calcined clay has been attracting growing interests as cement replacement due to its abundance on earth and wide availability. Compared to other calcined clay, kaolinite was identified as the most suitable SCM because of its high pozzolanic activity [6–9]. The reactive silica and alumina in the kaolinite will react with Portlandite to form cal-

* Corresponding author.
E-mail addresses: ceedhj@nus.edu.sg (H. Du), ceepsd@nus.edu.sg (S.D. Pang).

https://doi.org/10.1016/j.conbuildmat.2020.120152
0950-0618/

cium alumino-silicates hydrates C-A-S-H as well as calcium aluminate hydrates C-A-H [51]. These products can fill space and contribute to the development of concrete properties [10,11]. Furthermore, some recent research indicates that even the low-grade kaolin clay can constitute a potential source of high reactivity pozzolanic material [12,13]. This is an important finding since the majority clay deposits on the earth are not sufficiently pure to produce metakaolin (a very active pozzolan with minimum of 85% kaolinite). More recently, the novel usage of limestone calcined clay cement (or namely LC3) has drawn wide interests due to the even higher clinker replacement levels with comparable mechanical properties [3,14] in concrete. In this ternary blended binder system, alumina from calcined clay can react with limestone to produce carbonaluminate hydrates in addition to its pozzolanic reaction with Portlandite. The reaction can be expressed as follows [14]:

$$0.24C\bar{C}+5.02CH + AS_2 + (0.74+2x)H \rightarrow 0.48C_3A\left(C\bar{C}\right)_{0.5}H_{12} + 2C_{1.67}A_{0.27}SH_x$$

It is noted that the majority of the previous studies emphasized the influence of replacing cement by calcined clay and limestone in normal strength mortar and concrete [14–18]. There is limited study of using calcined clay and limestone in high-performance concrete (HPC) so far. HPC is typically used in high-rise structures and highway bridges that span long distances, as it is able to resist high compressive loads and enables reinforced or prestressed girders to span greater lengths than normal-strength concrete. With modern designs of buildings and infrastructures getting increasingly complex and unusual, the usage of HPC to achieve the structural requirements of these designs is set to increase. Furthermore, there is an aggressive push towards high-performance concrete to reduce the building footprint and increase the durability of the building to withstand more extreme weathering due to climate change. To reduce carbon emissions while catering to the trend of increasing HPC usage, it is thus worthwhile to study the combined usage of calcined kaolinite clay and limestone on HPC.

This study aims to determine the suitability of calcined clay (CC) and limestone (LS) as a combined cement substitute in HPC. The impact of such substitution was assessed in terms of blends reaction evolution and HPC properties at different ages regarding mechanical and durability performances in the long term. Locally available kaolin clay was used in this study. A preliminary study has revealed that the raw clay could have the highest pozzolanic reactivity after 800 °C thermal treatment and the optimum clay-to-limestone ratio is 2:1 by mass [10,19]. This study aims to shed light on the performance evaluation of HPC containing the combined calcined clay and limestone and the underlying mechanisms.

2. Materials and methods

2.1. Materials

The materials used in this study include CEM I 52.5 N ordinary Portland cement (OPC), limestone, crystalline quartz, kaolin clay, natural sand and crushed granite stone. The specific gravity of OPC, limestone, quartz and clay is 3.15, 2.83, 2.62 and 2.65, respectively, as determined by an Automatic Density Analyzer (ULTRAPYC 1200e). Limestone and quartz were supplied by a local chemical factory. Kaolin clay was purchased from Kaolin (Malaysia) SDN BHD, Malaysia. The kaolinite content in that clay determined by thermogravimetric analysis (TGA) is about 60% using the tangent method [20]. The weight loss of the raw clay with increasing temperature is presented in Fig. 1. The calcination process was performed by stacking clay-filled crucibles in a program

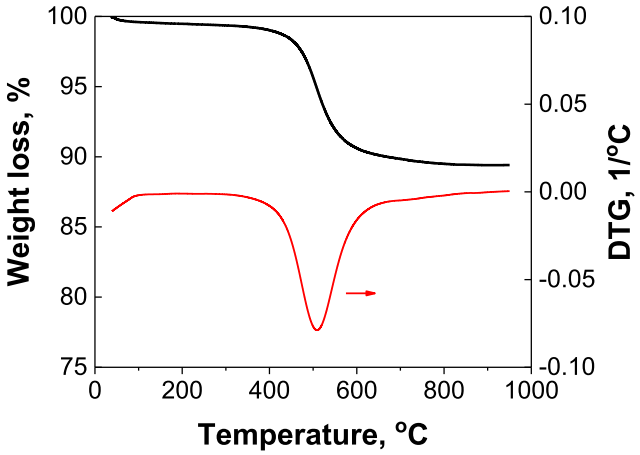

Fig. 1. Weight loss and derivative weight loss (DTG) curves for raw clay.

controlled furnace (ELLITE 1200 °C laboratory chamber furnace) and heating at a rate of 10 °C/min until 800 °C. That temperature was maintained for 1 h, after which the clays were removed from furnace immediately and spread on a metal plate to cool to ambient temperature. X-ray diffraction (XRD) technique was employed to detect the mineral phase change during the calcination using Shimadzu XRD-6000. The XRD patterns are shown in Fig. 2. It is noted that the raw material is a mixture of kaolinite, illite and quartz, instead of pure kaolin clay. After 800 °C of heating, peaks of kaolinite have almost disappeared, indicative of the decomposition of kaolinite. Previous literature has revealed that the pozzolanic reactivity of calcined clay originates from the structure disorder associated with the dehydroxylation [21]. Peaks corresponding to quartz and illite are still detectable, implying that CC still contains crystalline illite and quartz.

The chemical composition for OPC and CC were characterized by X-ray fluorescence (XRF) using PANalytical and shown in Table 1. The high content of potassium in the raw clay suggests the presence of illite, agreeing well with the XRD observation. Particle size distribution for powder materials are measured by Partica LA-950 laser diffraction analyzer and displayed in Fig. 3. River sand with a fineness modulus of 2.90 and 12.5 mm granite coarse aggregate were used to produce HPC concrete. Fig. 4**(a)** shows a typical blocky kaolinite in the as-received clay. It consists of pseudo-hexagonal crystals, stacking on top of one another. After 800 °C

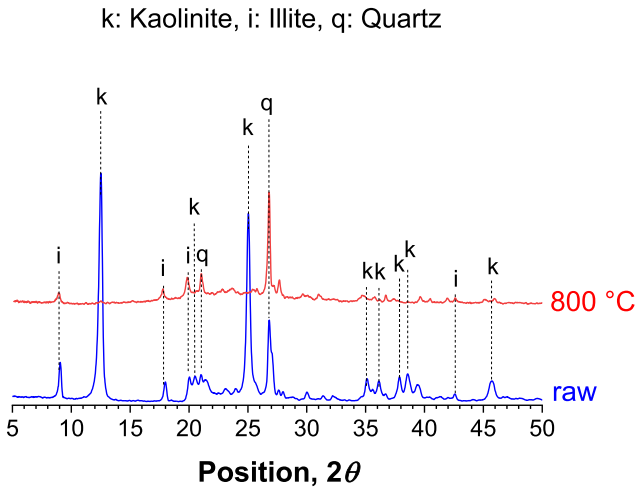

Fig. 2. XRD patterns for raw clay and calcined clay.

Table 1
Chemical composition for OPC, raw and calcined clay.

% weight	SiO_2	Al_2O_3	Fe_2O_3	CaO	MgO	SO_3	Na_2O	K_2O	TiO_2	Others
OPC	19.02	4.69	3.35	66.48	1.31	3.64	0.31	0.53	0.41	0.26
raw clay	56.30	37.42	1.20	0.02	0.46	0.08	0.07	3.51	0.69	0.25
calcined clay	54.79	40.10	1.38	0.03	0.40	0.03	0.06	2.19	0.67	0.35

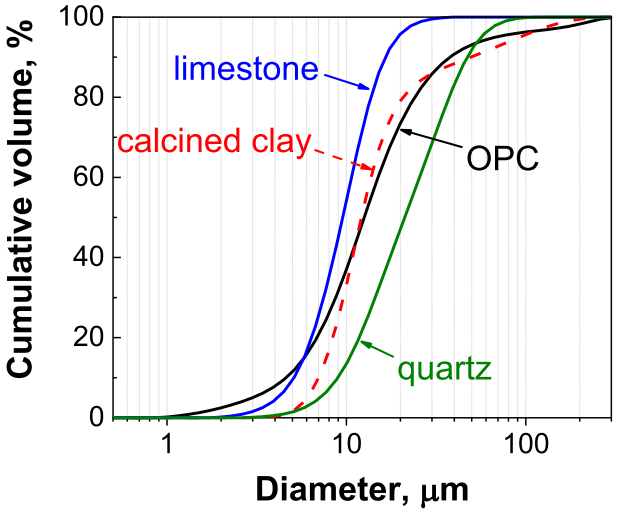

Fig. 3. Particle size distribution of OPC, calcined clay, limestone and quartz.

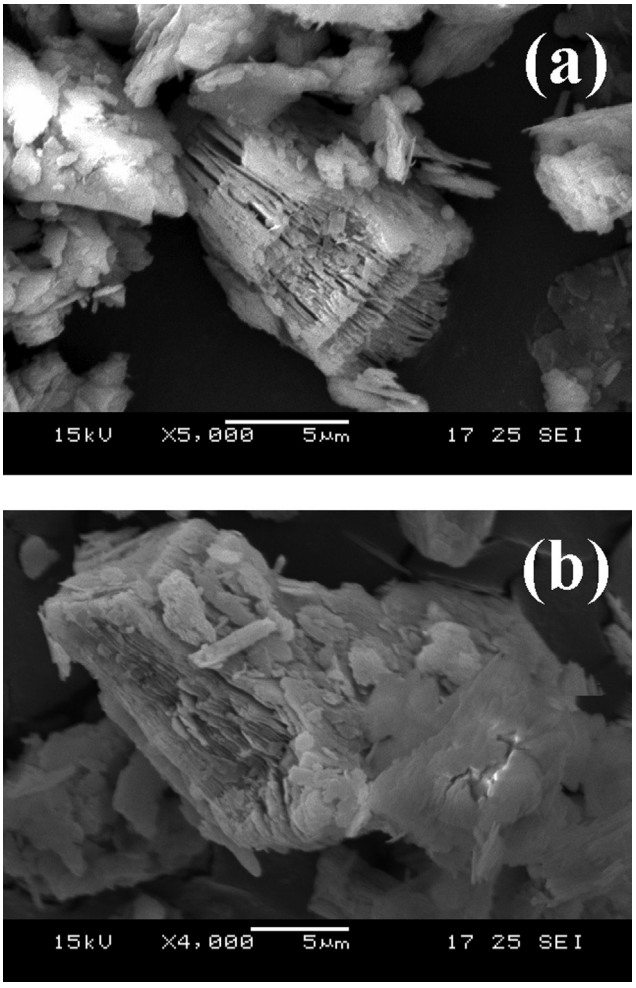

Fig. 4. SEM photos of (a) raw clay and (b) calcined clay.

thermal treatment, the morphology is slightly changed from SEM observation in Fig. 4**(b)**.

2.2. Mix proportion and casting

Mix proportion for HPC was selected according to ACI 363R [22], as listed in Table 2. Compared to the reference HPC, 30% and 45% cement content was substituted by the combined use of CC and LS (with a constant weight ratio of 2:1, as suggested by [14] and confirmed by [19]) in B30 and B45 mix, respectively. Water-to-cementitious materials (*w/cm*) ratio keeps at 0.30 for all the mixes. At the same time, two additional mixes, Q30 and Q45, were tested using quartz powder with equivalent weight of CC and LS, to assess the filler effect. Polycarboxylate-based superplasticizer (ADVA 181 N) was added for each mix to adjust the slump to be around 100 mm. Fresh concrete mixtures were poured in steel moulds and consolidated on a vibration table. Covered by plastic sheet for 24 h, concrete specimens were demolded and stored in a fog room (30 °C, 100% RH) until the testing age.

2.3. Test methods and specimens

Hydration studies were conducted on paste samples with the same *w/cm* ratio. The heat flow of the hydration was measured by an isothermal calorimeter (TAM Air from TA instrument). Cumulative heat of reaction was calculated starting from the lowest point of the dormant period. For each paste, two specimens were measured. Hydration of paste samples were stopped by immersing chunk samples in isopropanol for at least 3 days and vacuum drying for 1 day. The dried paste samples were ground to be finer than 75 μm for thermogravimetric analysis (TGA) and X-ray diffraction (XRD), at the age of 1, 3, 7, 28 days. TGA was performed on about 40 mg paste powder using DISCOVERY TGA from TA instrument. Weight loss was monitored for sample heated from 30 °C to 900 °C in N_2 atmosphere, at a rate of 10 °C/min. XRD measurements were conducted with Shimadzu XRD-6000 diffractometer. XRD scan was between 5° and 25°. Chemical shrinkage of paste was measured according to ASTM C 1608 [23], until 12 weeks. Autogenous shrinkage was assessed using paste samples in accordance with ASTM C 1698 [24]. For each mix, paste was cast in two corrugated polyethylene tubes and the deformation of each specimen was continuously monitored by LVDT until 10 days.

Elastic modulus and compressive strength of concrete were measured at 1, 3, 7, 28, 91 and 182 days, on 3 cylinders of Ø100 × 200 mm, according to ASTM C 469 [25] and C 39 [26], respectively. Water sorptivity, rapid chloride penetration test and rapid migration test were conducted for concrete at 28 and 182 days, on 3 disks of Ø100 × 50 mm, according to ASTM C 1585 [27], C 1202 [28] and NT BUILD 492 [29], respectively. Three concrete prisms of 75 × 75 × 285 mm were used to measure the drying shrinkage as per ASTM C 157 [30]. The specimens were stored in water for 1 week and followed by exposure to drying condition (RH 65%) until 1 year.

Table 2
Mix proportion of HPC (kg/m^3).

Mix	Water	OPC	Calcined Clay	Limestone	Quartz	Sand	Aggregate	SP (L/m^3)
OPC	145	480	–	–	–	715	1050	3.8
B30	145	336	96	48	–	715	1050	7.6
B45	145	264	144	72	–	715	1050	10.6
Q30	145	336	–	–	144	715	1050	3.8
Q45	145	264	–	–	216	715	1050	3.8

3. Results and discussion

3.1. Hydration

The cumulated heat for each gram of cement in different mixes, up to 15 days, is presented in Fig. 5. The reference OPC mix shows a rapid increase in the heat within the first 3 days of hydration while much slower increase after that, implying that the main hydration occurs in the first three days. For Q30 and Q45 mixes, the normalized heat increases with higher quartz replacement, due to the filler effect which could provide more space and available water for cement hydration. This consists well with previous findings [31,32]. For B30 and B45 mixes, the cumulated heat is even higher than Q30 and Q45 at the same cement replacement level. Assuming that the quartz filler is inert and that the physical effect it introduces is equivalent to that of the pozzolans (CC and LS in this study), the difference in the cumulated heat between the blended paste and the quartz filler paste represents the heat released from the pozzolanic and synergistic reaction. In this study, B45 exhibits the highest heat attributed to the combined effect of filler effect and pozzolanic reaction. It should also be noted that, up to 15 days, the additional reaction contributes more to the total heat in B30 mix than in B45 mix. It is also noted that the normalized hydration heat is less than the mix with higher *w/c* ratio of 0.50 [13]. This is because of the lower water dosage in this HPC mix, which restrains the full hydration of cement grains. RH in the mix would drop significantly due to the pozzolanic reaction of CC, which could slow down the clinker hydration at higher cement substitution level.

Chemical shrinkage of cement is induced by cement hydration and its magnitude is directly linked with the degree of cement hydration. The influence of replacing cement with the combined CC and LS on the chemical shrinkage, up to 84 days, is displayed in Fig. 6. All the mixes showed rapidly increasing chemical shrinkage within 7 days and much more gently afterwards. Compared to the reference paste, paste B30 and B45 both exhibited much higher chemical shrinkage, indicating more reaction occurs normalized to 1 g of cement. This is consistent with previous findings on the influence of metakaolin on chemical shrinkage of cement composites [33].

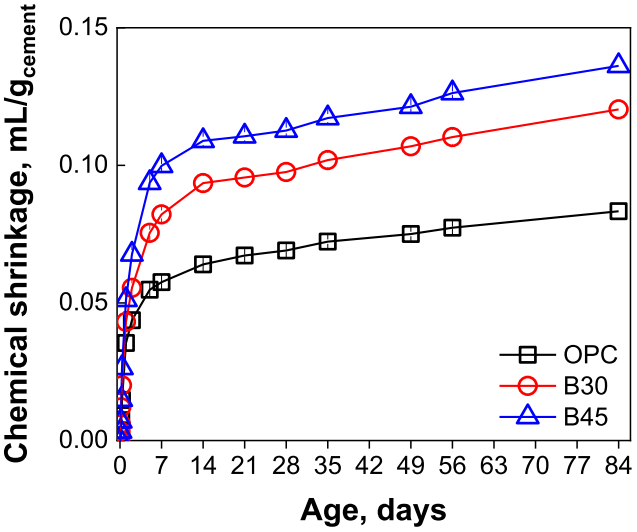

Fig. 6. Chemical shrinkage of different pastes.

XRD patterns for different pastes at 1, 7 and 28 days are shown in Fig. 7. Pure cement paste shows the formation of ettringite (E) and a growing Portlandite (CH) content from the first day. For B30 and B45 pastes, hemicarboaluminate (Hc) and monocarboaluminate (Mc) are formed on 7 and 28 days while the CH peak was weakened with age. It is also noted that peaks corresponding to

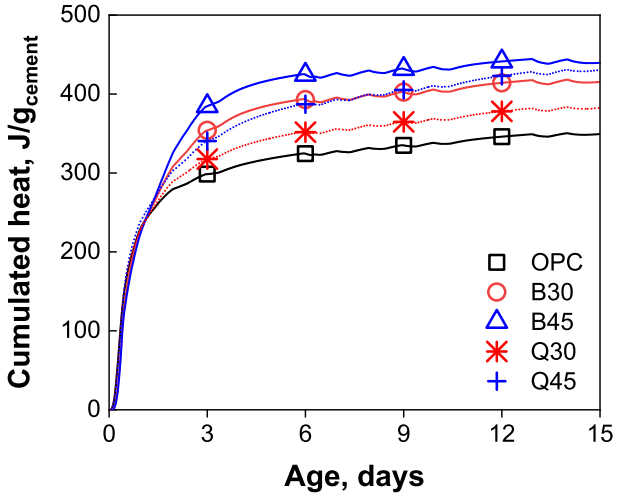

Fig. 5. Hydration of different pastes.

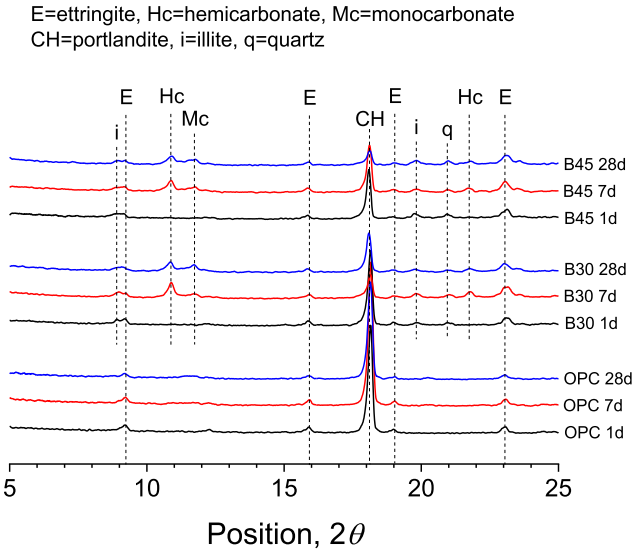

Fig. 7. XRD patterns for different pastes.

illite and quartz are detected for blended paste at each age, because the crystal phases hardly involved in the hydration. Hc appears at early hydration in limestone-containing cement and gradually converts to Mc [34]. Previous findings on the synergistic effect between limestone and fly ash have revealed that limestone could react with the aluminate phases provided by fly ash to form calcium carboaluminte hydrates, stabilizing the ettringite [35]. This synergy was reported to decrease the porosity of cement paste and enhance concrete properties [36]. Similar synergy between limestone and other aluminate-containing SCMs have been reported, for instance calcium aluminosilicate glass [37] and slag [38]. From Fig. 7, it is assumed that the active alumina and silicate phases in the CC form Hc, Mc and C-A-S-H hydrates, by reacting with limestone and Portlandite, consistent with **Eq. 1**. XRD patterns shows that this combined reaction would not occur before 1-day when no Hc or Mc peak was found. This agrees well with a previous report [14].

The portlandite content in the paste mix is displayed in Fig. 8, as determined from TGA method. For the pure cement paste, CH content continuously increases from 1 day to 91 days, with a much faster rate within the first week. The same trend was found for quartz-filling paste Q30 and Q45. Because of the diluted cement amount in those mixes, the total CH content is lower compared with the OPC mix. CH content in the blended paste exhibits an increase up to 3 days and drops a little at 7 days and stabilizes onwards. The gap between the blended mix and reference quartz mix (with the same cement substitution level) represents the amount of Portlandite consumed in the reaction with CC and LS, at each age. It is noted that CH content in the blended paste is higher than the quartz paste even on the first day, indicating that pozzolanic reaction of CC with Portlandite could start as early as from the first day. This gap in CH increases until 7-day and remains unchanged afterwards. The results may imply that the reaction of CC and LS might be almost completed within 7 days. A recent study shows the similar findings on the CH content in LC3 paste with a *w/cm* ratio of 0.40 [39]. Due to the lower *w/cm* ratio, water will be competed between cement hydration and the reaction of CC and LS as pointed by [31]. Hence, the reaction of CC and LS might be restricted compared to mixes with higher *w/cm* ratio. This can explain the more obvious decreasing CH content with curing age in a previous study on LC3 [14].

From the various measuring techniques, it can be concluded that the pozzolanic reaction of CC might start very quickly (as suggested from CH content) and its synergizing reaction with limestone will start occurring within the first week (as seen from XRD, Calorimetry and chemical shrinkage). As a result of the reactions, C-A-S-H and carbonaluminate hydrates are generated, as evidenced by XRD results.

3.2. Autogenous shrinkage

Fig. 9 shows the autogenous shrinkage of different paste mixes during the first 10 days. Autogenous shrinkage is a concern for HPC in which the hydration would result in great drop in RH and hence possibly shrinkage cracks. The autogenous shrinkage OPC paste increases fast in the first 3 days and then slowly increases until 10 days, reaching about 400 micro-strains. Paste with CC and LS also exhibit a rapid increase in autogenous shrinkage within the first day and an additional rapid increase between 2 and 5 days, as seen in Fig. 9. Kaolinite is high pozzolanic reactive and can start reacting with Portlandite before 1 day [40]. The rapid autogenous shrinkage on the first day might correspond with this pozzolanic reaction. At the same time, the high surface area and platy morphology of CC could absorb water, reducing the effective *w/c* ratio and increasing autogenous shrinkage [41]. The second rapid increase in autogenous shrinkage from 2 to 5 days might be caused by the synergistic reaction between CC and LS. Compared to OPC paste, blended paste has a higher potential to crack because of the higher autogenous shrinkage, approaching about 700 and 800 micro-strains for B30 and B45 mixes.

There is only one available literature reporting the autogenous shrinkage of LC3 cement paste with *w/cm* of 0.40 [42]. They found the incorporation of LS and CC actually decrease the autogenous shrinkage in the first month but increase it in the following month. This study firstly reports the autogenous shrinkage of low *w/cm* paste with CC and LS. The results obtained in this study show that the partial cement replacement increases the autogenous shrinkage at the early age.

3.3. Compressive strength and elastic modulus

The strength development for each HPC mix is displayed in Fig. 10**(a)**. All the mixes exhibited increasing compressive strength from 1 day to 6 months. At the age of 1 day, OPC mix showed an average strength of 46 MPa. Mixes B30 and Q30 showed almost identical strength of 30 MPa while mixes B45 and Q45 exhibited a compressive strength of 19 MPa. The lower strength than the reference OPC mix can be explained by the cement dilution effect. In

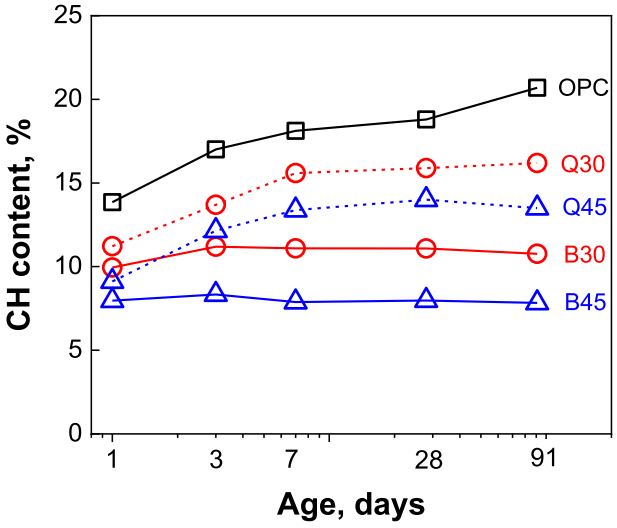

Fig. 8. CH content in different pastes.

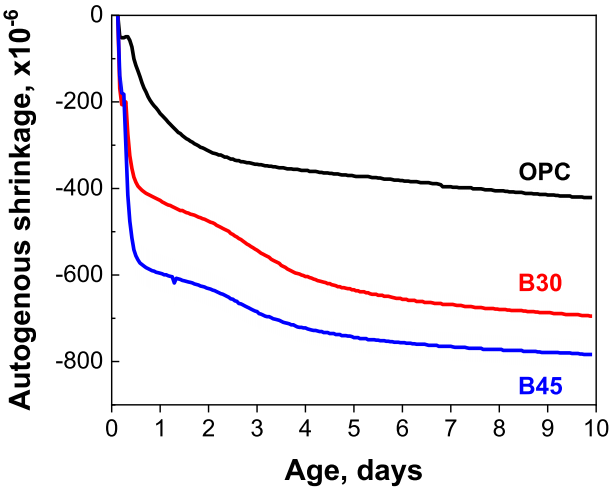

Fig. 9. Autogenous shrinkage of different pastes.

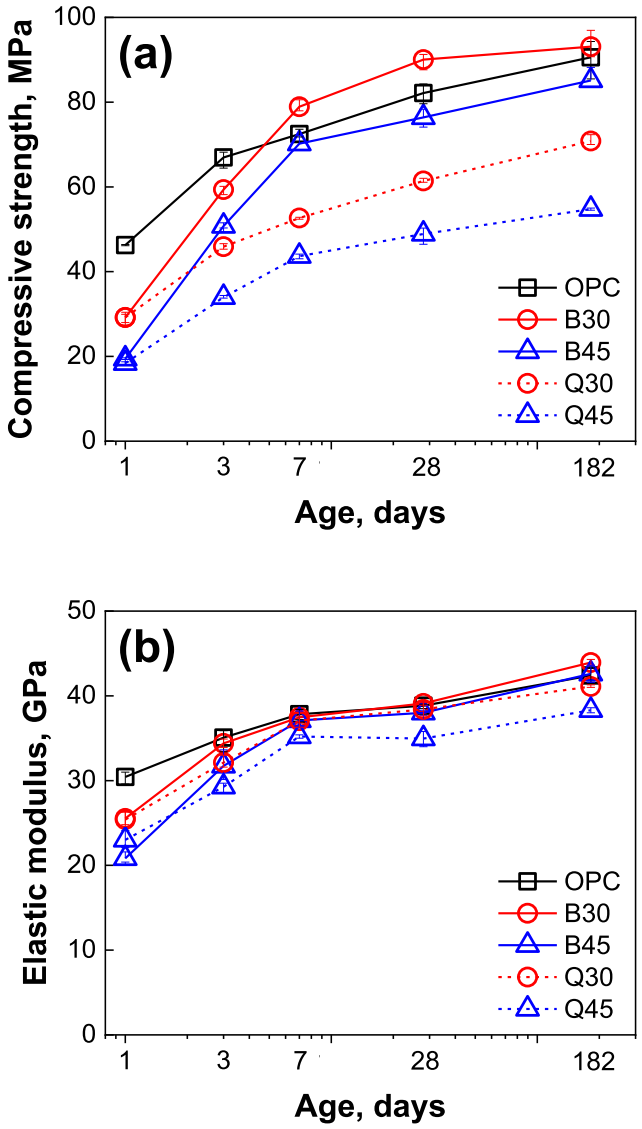

Fig. 10. (a) Compressive strength and (b) elastic modulus of different concrete mixes.

addition, the comparable strength between blended cement and quartz filler mixes implies that the pozzolanic reaction of kaolinite in the first day (which has been confirmed in Section 3.1) is not able to cause strength improvement. At the age of 3 days, the reference mix still shows the highest strength of 67 MPa. Mix Q30 and Q45 show compressive strength of 46 MPa and 34 MPa. It is interesting to note that the mix B30 and B45 showed a higher strength increase rate and reached 60 MPa and 50 MPa, much higher than Q30 and Q45, respectively. This trend is even more obvious at the age of 7 days when mix B30 shows the highest strength of 79 MPa while the reference mix shows a 72 MPa strength. Mix B45 has 7-day strength of 70 MPa, close to that of the reference mix. This can be attributed to the pozzolanic reaction of kaolinite in the clay and its synergizing action with limestone. Strength increase rate from 7 days to 182 days are almost the same for each mix, implying that the reaction of CC and LS might have been completed within the first week due to the limited amount of water for chemical reactions in the mix. This observation in compressive strength agrees well with the chemical reaction as discussed in the earlier section.

Elastic moduli of different HPC mixes are plotted in Fig. 10**(b)** at various testing ages. Within the first three days, the reference mix has the highest modulus while mix B30 and B45 increases faster than Q30 and Q45 due to the chemical reaction of CC and LS. From 7-day onwards, B30 and B45 show almost the same and even higher modulus than the reference mix while Q45 exhibits the lowest modulus at each age due to the cement replacement by inert quartz.

The increased compressive strength and elastic modulus for B30 and B45 mixes at later age could be attributed to the microstructural densification as a result of the reactions among Portlandite, CC and LS. Some recent studies have revealed that in the blended mixture of CC and LS paste, pore connectivity could be significantly reduced in addition to the capillary porosity refinement [39]. Due to the smaller *w/c* ratio, insufficient water is available for the full reaction among CC, LS and Portlandite. Therefore, the cement substitution of 30% shows a better mechanical performance rather than 45% in this study. This is slightly different with what have been reported for normal strength concrete [14].

Elastic modulus of concrete is primarily governed by the coarse aggregate (size, hardness and volume) as well as cement paste properties. In this study, the only variable is the binder composition among all the mixes. Hence, the change in elastic modulus is only caused by the cement replacement by CC and LS or Qz. The general observation is that denser binder microstructures result in higher strength and higher elastic modulus. However, this change is more pronounced in compressive strength rather than in elastic modulus. This is consistent with previous findings [43,44].

3.4. Drying shrinkage

Drying shrinkage of different HPC mixes are displayed in Fig. 11 up to 182 days. The reference concrete mix shows a continuously increasing drying shrinkage with longer period and reaches 365 micro-strains. There is no much difference in the drying shrinkage between B30 and B45 mix. They both show 240 micro-strains at 182 days of drying. This finding indicates that the blended CC and LS concrete mixes can have reduced drying shrinkage, possibly due to the reaction of CC and LS which could cause (1) less amount of water to escape from concrete, and (2) refined pore structure which easily hinders the movement of moisture outwards. Metakaolin, as cement replacement, has been reported to be able to reduce shrinkage of concrete because of the refined pore structure

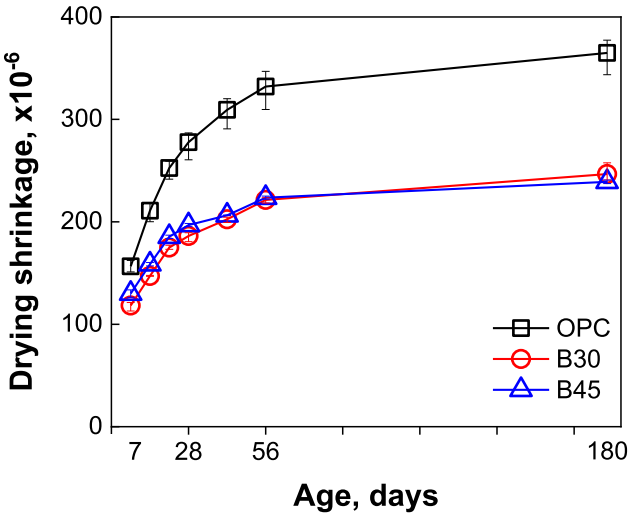

Fig. 11. Drying shrinkage of different concrete mixes.

[45,46]. This is the first study to evaluate the shrinkage performance of HPC made with CC and LS as partial cement substitution. A recent study reports that a mortar mix with CC and LS (as 45% cement replacement) exhibited slightly higher shrinkage than pure OPC mortar [17]. The reason might be due to the higher *w/cm* ratio used in the CC mortar for the same consistency in that study.

3.5. Water sorptivity

Fig. 12 demonstrates the influence of blended CC and LS on the initial water sorptivity of concrete, at both 28 and 182 days. The initial water sorptivity decreases with longer curing age for each mix, due to the microstructural evolution associated with continuous cement hydration. At 28-day, OPC mix has the highest water sorptivity of approximately 3×10^{-4} mm/s$^{0.5}$. The replacement of 30% and 45% of blend CC and LS can significantly reduce the sorptivity by about 55%. Similar reducing trend in sorptivity could be observed on 182 days. Sorptivity is an important index to evaluate the resistance of concrete against moisture ingress by capillary absorption. Previous works have found that sorptivity of cement composites is mainly governed by the pore network (total porosity, pore size and connectivity) which provides the pathways for moisture [47]. The incorporation of blended CC and LS is expected to densify the interfacial transition zone (ITZ) between aggregates and cement matrix as well as refine the pore structures for the bulk paste. The results obtained in this study agrees well with a recent work [17] which conducted the mercury intrusion porosimetry test to confirm the refined critical pore diameter in LC3 concrete. This refined pore network will partially block the transport paths for moisture.

3.6. Electrical conductivity

Fig. 13 shows the influence of the blended CC and LS on the RCPT result at both 28 and 182 days. In this study, RCPT is interpreted as the electrical conductivity rather than an indicator for concrete's resistance against chloride ions. At each age, the reference concrete mix shows the highest electrical conductivity while the addition of CC and LS significantly decreases the conductivity. The difference between 30% and 45% cement replacement level is marginal. For a saturated concrete, its electrical conductivity is dominated by its pore structures and pore solution chemistry. As mentioned in the earlier section, the reactions of CC and LS will refine the pore structure and lead to a more torturous routes for the transport of ions in the pore solution. At the same time, the combination of CC and LS consumes calcium hydroxide to form C-A-S-H hydrates which could also uptakes alkalis (Na^+ and K^+). This reduces the concentration of ions in the pores solution. A direct evidence on the ions concentration reduction in the cement pore solution has been provided by a recent study [39]. Therefore, the simultaneous action of refined structure and reduced ion concentration can greatly decrease the electrical conductivity of concrete. The large drop in electrical conductivity has also been well documented for pozzolans like fly ash or glass powder [48,49].

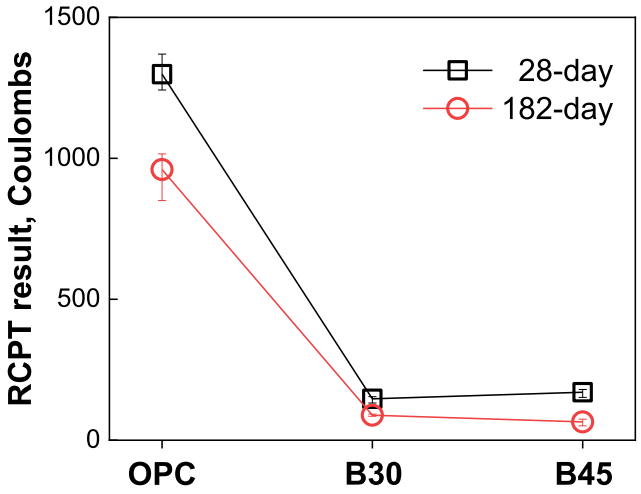

Fig. 13. RCPT results of different concrete mixes.

3.7. Resistance against chloride-ion

The effect of combined use of CC and LS on the rapid chloride migration coefficient is illustrated in Fig. 14, at both 28 and 182 days. Each concrete mix has higher resistance against chloride-ion (lower migration coefficient) from 28 to 182 days because of the cement hydration. At each testing age, the reference concrete mix has the highest chloride migration coefficient. 30% cement replacement leads to a great drop in the migration coefficient while 45% cement replacement does not cause further decrease but nevertheless much lower than the reference mix. Similar observation was found for 182-day result. Compared to

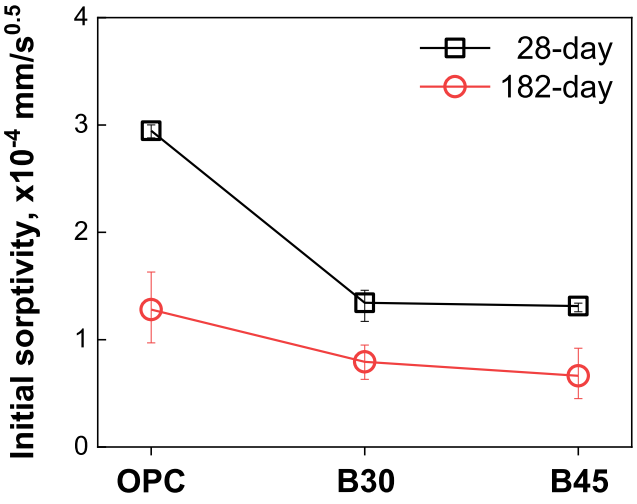

Fig. 12. Sorptivity of different concrete mixes.

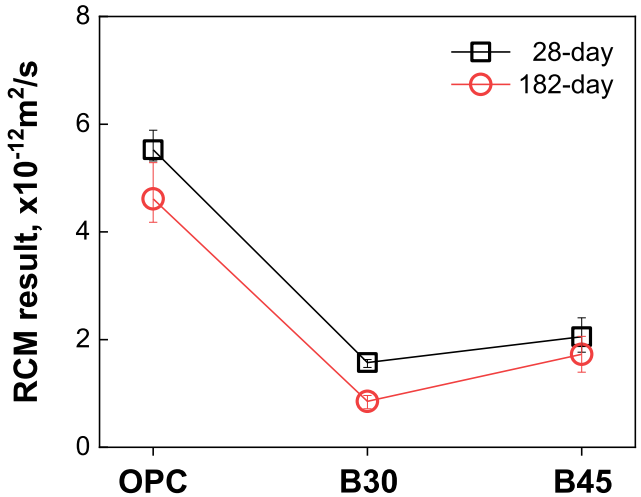

Fig. 14. Chloride resistance of different concrete mixes.

the pure OPC system, the blended binder concrete is more refined and densified, attributed to the reactions of limestone and calcined clay. In addition, the formed C-A-S-H gels have higher chloride-binding capacity due to the presence of alumina [50]. These two factors would contribute to a higher resistance against chloride-ion. A similar result was reported by [17] for normal strength concrete. However, the higher cement replacement at 45% slightly compromised this improvement because of the insufficient reactions among cement hydration products with CC and LS. This is consistent with the compressive strength whose improvement is most obvious at 30% cement substitution level.

4. Conclusions

This study aims to evaluate the hydration and properties of high-performance concrete incorporating calcined clay and limestone as partial cement replacement. A locally available medium kaolinite-content clay was used to produce the calcined clay. The following conclusion can be drawn:

(1) Pozzolanic reaction of calcined clay may start within the first day and its synergistic action with limestone starts from a little later stage. These reactions consume Portlandite and produce C-A-S-H gels and carbonaluminate phases. The reactions release additional heat and cause higher autogenous shrinkage. Results also reveal that the reaction might be completed within the first week due to the limited water amount in the low *w/cm* paste system.
(2) Mechanical properties of concrete with blended binder are lower than those of the reference pure cement mix in the first 3 days but grow faster and become comparable from 7 days onwards. This is particularly obvious for 30% cement replacement level.
(3) Transport of moisture, liquid and chloride ions is greatly hindered, mainly because of the refined pore structures in the blended binder concrete. Hence, drying shrinkage, water sorptivity, electrical conductivity and chloride permeability are all reduced from the pure cement concrete mix.

To the authors' best knowledge, this is the first comprehensive study on HPC containing CC and LS. The results reveal that 30% and 45% replacements both exhibit comparable mechanical properties and superior durability performances. Future study shall focus on the optimum design on the binder. For instance, the sulfate content and the ratio between CC and LS as well as the consistency of fresh concrete.

CRediT authorship contribution statement

Hongjian Du: Conceptualization, Methodology, Software, Validation, Investigation, Writing - original draft. **Sze Dai Pang:** Conceptualization, Methodology, Writing - review & editing, Funding acquisition.

Declaration of Competing Interest

The authors declare that they have no known competing financial interests or personal relationships that could have appeared to influence the work reported in this paper.

Acknowledgements

The authors wish to acknowledge the Singapore Ministry of Education (Grant Number R-302-000-183-114) for financial support. The authors wish to express their gratitude to Ms. Quek Xian Yun who accomplished numerous experiments during her final year project at the National University of Singapore. Great assistance from Mr. Ang Beng Oon and Ms. Li Wei of Concrete Laboratory is kindly acknowledged. The authors are grateful to Dr. Chew Soon Hoe and Mr. Seow Soon Leong for their help with the operation of laser diffraction analyzer in Geotechnical Engineering Laboratory.

References

[1] V.W.Y. Tam, A. Butera, K.N. Le, W. Li, Utilising CO2 technologies for recycled aggregate concrete A critical review, Constr. Build. Mater. 250 (2020), https://doi.org/10.1016/j.conbuildmat.2020.118903 118903.
[2] B. Lothenbach, K. Scrivener, R.D. Hooton, Supplementary cementitious materials, Cem. Concr. Res. 41 (2011) 217–229, https://doi.org/10.1016/j.cemconres.2010.12.001.
[3] T.R. Muzenda, P. Hou, S. Kawashima, T. Sui, X. Cheng, The role of limestone and calcined clay on the rheological properties of LC3, Cem. Concr. Comps. 107 (2020), https://doi.org/10.1016/j.cemconcomp.2020.103516 103516.
[4] B. Nematollahi, J. Sanjayan, F.U.A. Shaikh, Synthesis of heat and ambient cured one-part geopolymer mixes with different grades of sodium silicate, Ceram. Int. 41 (2015) 5695–5704, https://doi.org/10.1016/j.ceramint.2014.12.154.
[5] M.J. Shannag, A. Yeginobali, Properties of pastes, mortars and concretes containing natural pozzolan, Cem. Concr. Res. 25 (1995) 647–657, https://doi.org/10.1016/0008-8846(95)00053-F.
[6] C. He, B. Osbaeck, E. Makovicky, Pozzolanic reactions of six principal clay minerals: Activation, reactivity assessments and technological effects, Cem. Concr. Res. 25 (1995) 1691–1702, https://doi.org/10.1016/0008-8846(95)00165-4.
[7] R. Fernandez, F. Martirena, K.L. Scrivener, The origin of the pozzolanic activity of calcined clay minerals: A comparison between kaolinite, illite and montmorillonite, Cem. Concr. Res. 41 (2011) 113–122, https://doi.org/10.1016/j.cemconres.2010.09.013.
[8] S. Hollanders, R. Adriaens, J. Skibsted, O. Cizer, K. Elsen, Pozzolanic reactivity of pure calcined clay, App. Clay. Sci. 132–133 (2016) 552–560, https://doi.org/10.1016/j.clay.2016.08.003.
[9] J. Lapeyre, H. Ma, A. Kumar, Effect of particle size distribution of metakaolin on hydration kinetics of tricalcium silicate, J. Am. Ceram. Soc. 102 (2019) 1–13, https://doi.org/10.1111/jace.16467.
[10] F. Avet, E. Boehm-Courjault, K. Scrivener, Investigation of C-A-S-H composition, morphology and density in limestone calcined clay cement (LC^3), Cem. Concr. Res. 115 (2019) 70–79, https://doi.org/10.1016/j.cemconres.2018.10.011.
[11] H. Maraghechi, F. Avet, H. Wong, H. Kamyab, K. Scrivener, Performance of limestone calcined clay cement (LC3) with various kaolinite contents with respect to chloride transport, Mater. Struct. 51 (2018) 125, https://doi.org/10.1617/s11527-019-1415-0.
[12] A. Alujas, R. Fernandez, R. Quintana, K.L. Scrivener, F. Martirena, Pozzolanic reactivity of low grade kaolinitic clays: influence of calcination temperature and impact of calcination products on OPC hydration, App. Clay Sci. 108 (2015) 94–101, https://doi.org/10.1016/j.clay.2015.01.028.
[13] H. Du, S.D. Pang, Value-added utilization of marine clay as cement replacement for sustainable concrete production, J. Clean Prod. 198 (2018) 867–873, https://doi.org/10.1016/j.jclepro.2018.07.068.
[14] M. Antoni, J. Rossen, F. Martirena, K.L. Scrivener, Cement substitution by a combination of metakaolin and limestone, Cem. Concr. Res. 42 (2012) 1579–1589, https://doi.org/10.1016/j.cemconres.2012.09.006.
[15] Scrivener KL, Favier A (2015) Calcined clays for sustainable concrete, Proceedings of the 1st International Conference on Calcined Clays for Sustainable Concrete. Springer.
[16] Martirena F, Favier A, Scrivener KL (2017) Calcined clays for sustainable concrete, Proceedings of the 2nd International Conference on Calcined Clays for Sustainable Concrete. Springer.
[17] Y. Dhandapani, T. Sakthivel, M. Santhanam, R. Gettu, R.G. Pillai, Mechanical properties and durability performance of concretes with Limestone Calcined Clay Cement (LC^3), Cem. Concr. Res. 107 (2018) 136–151, https://doi.org/10.1016/j.cemconres.2018.02.005.
[18] Y. Dhandapani, M. Santhanam, Assessment of pore structure evolution in the limestone calcined clay cementitious system and its implications for performance, Cem. Concr. Compos. 84 (2017) 36–47, https://doi.org/10.1016/j.cemconcomp.2017.08.012.
[19] H Du, A Dixit, SD Pang, in: S. Bishnoi (Ed.), Calcined Clays for Sustainable Concrete. RILEM Bookseries, 25, Springer, Singapore, 2020. https://doi.org/10.1007/978-981-15-2806-4_7.
[20] Fernandez R (2009) Calcined clayey soils as a potential replacement for cement in developing countries. Dissertation, EPFL.
[21] R. Siddique, J. Klaus, Influence of metakaolin on the properties of mortar and concrete: A review, App. Clay Sci. 43 (2009) 392–400, https://doi.org/10.1016/j.clay.2008.11.007.
[22] A.C.I. Committee 363, Report on High-Strength Concrete American Concrete Institute 2010
[23] ASTM C1608-17, Standard Test Method for Chemical Shrinkage of Hydraulic Cement Paste, ASTM International, West Conshohocken, PA, 2017.

[24] ASTM C1698–19(2019), Standard, Test Method for Autogenous Strain of Cement Paste and Mortar, ASTM International, West 2014 Conshohocken, PA
[25] ASTM C469/C469M-14, Standard Test Method for Static Modulus of Elasticity and Poisson's Ratio of Concrete in Compression, ASTM International, West 2014 Conshohocken, PA
[26] ASTM C39/C39M-17b, Standard Test Method for Compressive Strength of Cylindrical Concrete Specimens, ASTM International, West Conshohocken, PA, 2017
[27] ASTM C1585-13, Standard Test Method for Measurement of Rate of Absorption of Water by Hydraulic-Cement Concretes, ASTM International, West Conshohocken, PA, 2013.
[28] ASTM C1202-17, Standard Test Method for Electrical Indication of Concrete's Ability to Resist Chloride Ion Penetration, ASTM International, West Conshohocken, PA, 2017.
[29] N.T. Build 443, Concrete, Hardened: Accelerated Chloride Penetration 1995 NORDTEST, Espoo
[30] ASTM C157/C157M-08, Standard Test Method for Length Change of Hardened Hydraulic-Cement Mortar and Concrete, ASTM International, West Conshohocken, PA, 2014.
[31] W. Huang, H. Kazemi-Kamyab, W. Sun, K.L. Scrivener, Effect of cement substitution by limestone on the hydration and microstructural development of ultra-high performance concrete (UHPC), Cem. Concr. Compos. 77 (2017) 86–101, https://doi.org/10.1016/j.cemconcomp.2016.12.009.
[32] Y.H. Kwon, S.H. Kang, S.G. Hong, J. Moon, Intensified pozzolanic reaction on kaolinite clay-based mortar, App. Sci. 7 (2017) 522, https://doi.org/10.3390/ma10030225.
[33] W. Yodsudjai, K. Wang, Chemical shrinkage behavior of pastes made with different types of cements, Constr. Build. Mater. 40 (2013) 854–862, https://doi.org/10.1016/j.conbuildmat.2012.11.053.
[34] A. Ipavec, Vuk T GabrovsekR, V. Kaucic, J. Macek, Carboaluminate phases formation during hydration of calcite-containing Portland cement, J. Am. Ceram. Soc. 94 (2011) 1238–1242, https://doi.org/10.1111/j.1551-2916.2010.04201.x.
[35] K. De Weerdt, M. Ben Haha, G. Le Saout, K.O. Kjellsen, H. Justnes, B. Lothenbach, Hydration mechanisms of ternary Portland cements containing limestone powder and fly ash, Cem. Concr. Res. 41 (2011) 279–291, https://doi.org/10.1016/j.cemconres.2010.11.014.
[36] K. De Weerdt, K.O. Kjellsen, E. Sellevold, H. Justnes, Synergy between fly ash and limestone powder in ternary cements, Cem. Concr. Compo. 33 (2011) 30–38, https://doi.org/10.1016/j.cemconcomp.2010.09.006.
[37] M. Moesgaard, D. Herfort, M. Steenberg, L.F. Kirkegaard, Y. Yue, Physical performances of blended cements containing calcium aluminosilicate glass powder and limestone, Cem. Concr. Res. 41 (2011) 359–364, https://doi.org/10.1016/j.cemconres.2010.12.005.
[38] G. Menendez, V. Bonavetti, E.F. Irassar, Strength development of ternary blended cement with limestone filler and blast-furnace slag, Cem. Concr. Compos. 25 (2003) 61–67, https://doi.org/10.1016/S0958-9465(01)00056-7.
[39] F. Avet, K.L. Scrivener, Investigation of the calcined kaolinite content on the hydration of Limestone Clay Cement (LC^3), Cem. Concr. Res. 107 (2018) 124–135, https://doi.org/10.1016/j.cemconres.2018.02.016.
[40] B.B. Sabir, S. Wild, J. Bai, Metakaolin and calcined clays as pozzolans for concrete: a review, Cem. Concr. Compos. 23 (2001) 441–454, https://doi.org/10.1016/S0958-9465(00)00092-5.
[41] X. Gao, S. Kawashima, X. Liu, S.P. Shah, Influence of clays on the shrinkage and cracking tendency of SCC, Cem. Concr. Compos. 34 (2012) 478–485, https://doi.org/10.1016/j.cemconcomp.2012.01.002.
[42] Ston J, Hilaire A, Scrivener K (2017) Autogenous shrinkage and creep of limestone and calcined clay based binders, in: Proceedings of the 2nd International Conference on Calcined Clays for Sustainable Concrete, Cuba, pp 447-454. https://doi.org/10.1007/978-94-024-1207-9_72
[43] R.P. Khatri, V. Sirivivatnanon, W. Gross, Effect of different supplementary cementitious materials on mechanical properties of high performance concrete, Cem. Concr. Res. 25 (1995) 209–220, https://doi.org/10.1016/0008-8846(94)00128-L.
[44] H.H. Nassif, H. Najm, N. Suksawang, Effect of pozzolanic materials and curing methods on the elastic modulus of HPC, Cem. Concr. Compos. 27 (2005) 661–670, https://doi.org/10.1016/j.cemconcomp.2004.12.005.
[45] M.H. Zhang, V.M. Malhotra, Characteristics of a thermally activated alumino-silicate pozzolanic material and its use in concrete, Cem. Concr. Res. 25 (1995) 1713–1725, https://doi.org/10.1016/0008-8846(95)00167-0.
[46] J.T. Ding, Z. Li, Effects of metakaolin and silica fume on properties of concrete, ACI Mater. J. 99 (2002) 393–398.
[47] E.J. Garboczi, Permeability, diffusivity, and microstructural parameters: A critical review, Cem. Concr. Res. 20 (1990) 591–601, https://doi.org/10.1016/0008-8846(90)90101-3.
[48] T.R. Naik, S.S. Singh, M.M. Hossain, Permeability of concrete containing large amounts of fly ash, Cem. Concr. Res. 24 (1994) 913–922, https://doi.org/10.1016/0008-8846(94)90011-6.
[49] H. Du, K.H. Tan, Properties of high volume glass powder concrete, Cem. Concr. Compos. 75 (2017) 22–29, https://doi.org/10.1016/j.cemconcomp.2016.10.010.
[50] R.K. Dhir, M.R. Jones, Development of chloride-resisting concrete using fly ash, Fuel 78 (1999) 137–142, https://doi.org/10.1016/S0016-2361(98)00149-5.
[51] J Dang, H Du, SD Pang, Hydration, strength and microstructure evaluation of eco-friendly mortar containing waste marine clay, Journal of Cleaner Production 272 (2020), https://doi.org/10.1016/j.jclepro.2020.122784 122784.